Multilead ECG Delineation Using Spatially Projected Leads From Wavelet Transform Loops

Rute Almeida*, Juan Pablo Martínez, Ana Paula Rocha, *Member, IEEE*, and Pablo Laguna, *Senior Member, IEEE*

***Abstract*—In this paper, a novel multilead (ML) based automatic strategy for delineation of ECG boundaries is proposed and evaluated with respect to the QRS and T-wave boundaries. The ML strategy is designed from a single-lead (SL) wavelet-transform-based delineation system. It departs from three orthogonal leads and takes advantage of the spatial information provided using a derived lead better fitted for delineation. SL delineation is then applied over this optimal derived lead. The ML strategy produces a reduced error dispersion compared to SL results, thus providing more robust, accurate, and stable boundary locations than any electrocardiographic lead by itself and outperforming strategies based on lead selection rules after SL delineation.**

***Index Terms*—Derived lead, loop, multilead (ML) ECG, vectocardiogram (VCG), wave delineation, wavelet transform (WT).**

I. Introduction

THE DIFFERENT phases of the heart's electrical activity are mapped to the waves in the ECG, typically known as P, Q, R, S, and T waves. The delineation of the ECG characteristic waves in each cardiac beat consists of detecting their peaks and boundaries (onset and end), and it also provides fundamental features to derive clinically useful information, namely about the duration of the electrical phenomena and their beat-to-beat evolution.

The detection of the QRS complex is the first and the most straightforward stage of any delineation system. The beat location is defined by the mark of the QRS complex main wave (usually the R wave), and the search for peaks and boundaries of the ECG waves is usually performed within temporal windows referred to the QRS position. Especially problematic due to the low SNR is the delineation of low-amplitude smooth wave boundaries, as it is usually the case of the T-wave end. Furthermore, there are no standard clear rules to locate the waves' boundaries, and this makes systematizing the delineation more difficult. Automatic methodologies allow one to avoid intra-/interobserver variability, and therefore, developing accurate and robust methods for ECG automatic delineation is a topic of main interest. A wide diversity of algorithms for QRS detection and different delineation approaches have been proposed, regarding some or all of the ECG waves and limits. In particular, an automatic single-lead (SL) delineation system, which generalizes the wavelet transform (WT) based methodology of [1], was presented in [2]. The method in [2] is able to determine and locate the peaks and boundaries of the QRS complex (namely identifying its individual waves), and of P and T waves. We refer to the ability of the algorithm to deal with various P and T wave morphologies, namely positive, inverted, biphasic, accounting for different morphologies. The WT provides a description of the signal in the time-scale domain, thereby allowing the representation of its temporal features at different resolutions (scales) according to their frequency content. Thus, regarding the purpose of locating different waves with typical frequency characteristics, the WT is a suitable tool for ECG automatic delineation.

According to the dipolar hypothesis, the electrical activity of the heart can be approximated by a time-variant electrical dipole, called the *electrical heart vector* (EHV). Thus, the voltage measured at a given lead would be the projection of the EHV into the unitary vector defined by the lead axis [3]. Choosing a particular lead for ECG delineation determines a point of view over the cardiac phenomena, and different latencies on the waves' onsets and ends are found in different leads. Nevertheless, the onset and end of the cardiac electric phenomena are indeed unique, and therefore, a global feature for all the leads. Thus, adequately combining the information provided by multiple leads is essential for the correct location of lead-independent waves' boundaries. The SL system [2] includes postprocessing decision rules to deal with multilead (ML) files by choosing global marks based on the SL-based sets of locations. However, this system is not truly ML, and it requires to apply the SL methodology to a large number of leads.

In this paper, an actual ML methodology regarding boundaries location is proposed and validated. The ML approach departs from the SL system and attends to the spatial characteristics of the different available leads, aiming to achieve a more robust delineation. This ML system was partially validated and

Manuscript received October 27, 2008; revised February 20, 2009 and April 2, 2009. First published May 12, 2009; current version published July 15, 2009. This work was supported in part by project TEC2007-68076-c02-02 from the Ministry of Science and Innovation and European Regional Development Fund (FEDER), Grupo Consolidado Communications Technology Group (GTC) from Diputación General de Aragón (DGA) T:30, and Centro de Matemática da Universidade do Porto (CMUP), financed by Foundation for Science and Technology, from the portuguese Fundação para a Ciência e a Tecnologia (FCT), Portugal, through the programmes POCTI and POCI 2010, with national and European Community Structural Funds. *Asterisk indicates corresponding author*.

*R. Almeida is with the Centro de Investigación Biomédica en Red en Bioingeniería, Biomateriales y Nanomedicina (CIBER-BBN), 50018 Zaragoza, Spain, and also with the Communications Technology Group (GTC), Aragón Institute of Engineering Research (I3A), University of Zaragoza, 50018 Zaragoza, Spain. He is also with the Centro de Matemática da Universidade do Porto (CMUP), Rua Campo Alegra 687, 4169-007 Porto, Portugal (e-mail: rbalmeid@unizar.es).

J. P. Martínez and P. Laguna are with the Communications Technology Group (GTC), Aragón Institute of Engineering Research (I3A), University of Zaragoza, 50018 Zaragoza, Spain, and also with the Centro de Investigación Biomédica en Red en Bioingeniería, Biomateriales y Nanomedicina (CIBER-BBN), 50018 Zaragoza, Spain (e-mail: jpmart@unizar.es; laguna@unizar.es).

A. P. Rocha is with the Departamento de Matemàtica Aplicada, Faculdade de Ciências da Universidade do Porto, 4169-007 Porto, Portugal, and also with the Centro de Matemàtica da Universidade do Porto (CMUP), 4169-007 Porto, Portugal (e-mail: aprocha@fc.up.pt).

Digital Object Identifier 10.1109/TBME.2009.2021658

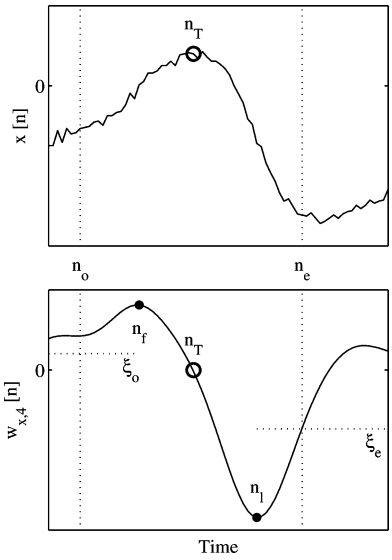

Fig. 1. Example of SL delineation of T-wave boundaries: n_{T} denotes T-wave peak (zero crossing of the WT), n_f and n_l the first and last significant WT slopes associated with the T wave, n_o and n_e the T-wave onset and end, and ξ_o and ξ_e the thresholds for T-wave boundaries. Note that T-wave end is marked using criterion 1) while T-wave onset satisfies criterion 2).

compared with other approaches as part of the "PhysioNet/ computers in cardiology challenge 2006: QT interval measurement" competition [4].

II. Materials and Methods

A. SL Delineation

The SL-based delineation system is described in detail elsewhere [2], and only general features are referred to here. The discrete dyadic WT is implemented using the algorithm *àtrous* to maintain temporal resolution at different scales. The wavelet-equivalent filter for each scale is resampled to keep the frequency band response independent of the sampling frequency of the ECG signal. The detection of the fiducial points is carried out across the adequate WT scales, attending to the dominant frequency components of each ECG wave: QRS waves correspond to a simultaneous effect in scales 2^1–2^4, while the T and P waves affect mainly scales 2^4 or 2^5. The prototype wavelet used (a derivative of a smoothing function) allows to obtain a WT at scale 2^m, $w_{x,m}[n]$, which is proportional to the derivative of the filtered version of the signal $x[n]$ with a smoothing impulse response at scale 2^m. Thus, ECG wave peaks correspond to zero crossings in the WT, and ECG maximum slopes correspond to WT's maxima and minima.

Depending on the number and polarity of the slopes found, a wave morphology is assigned and boundaries are located using threshold-based criteria. The onset (end) of a wave, $n_o(n_e)$, occurs before (after) the first (last) significant slope associated with the wave (the first (last) maximum of $|w_{x,m}[n]|$), at sample $n_f(n_l)$ (Fig. 1). Each boundary is located by selecting the sample nearest to n_f (n_l) where one of the following two criteria is satisfied (Fig. 1): 1) $|w_{x,m}[n]|$ is below a threshold $\xi_o(\xi_e)$ relative to $w_{x,m}[n_f]$ $(w_{x,m}[n_l])$ and 2) a local minimum of $|w_{x,m}[n]|$ exists before n_{f} (after n_{l}).

B. SL Selection Rule for ML Signals

To deal with ML signals and obtain global marks for peak location, a median postprocessing selection rule over SL-based locations is used. For boundaries location, the possibly different latencies between leads resulting from their spatial orientation need to be taken into account. Thus, the postprocessing rules for boundaries consist of ordering the SL annotations and selecting as the onset (end) of a wave the first (last) annotation whose k nearest neighbors lay within a δ ms interval. To combine 12 SL annotations, $\mathsf{k} = 3$, $\delta = 10$ ms were used for QRS end, and $\delta =$ 12 ms for QRS onset and T end [5].

C. ML Delineation

The ML delineation system proposed here considers three simultaneous orthogonal leads: $x[n], y[n],$ and $z[n]$. The vectocardiogram (VCG) is an EHV's canonical representation defined by three orthogonal leads [3], which are usually acquired as the corrected Frank leads, and is given by

$$\mathbf{s}[n] = [x[n], y[n], z[n]]^T. \tag{1}$$

An example of a beat according to the Frank leads and the respective VCG spatial loop for a T wave is plotted in Fig. 2(a) and (c).

A spatial WT *loop* in a time window W is given by

$$\mathbf{w}_m[n] = [w_{x,m}[n], w_{y,m}[n], w_{z,m}[n]]^T \tag{2}$$

for a given scale $2^m \big|_{m\in\{1,2,3,\ldots\}}$, as illustrated in Fig. 2(b) and (d). As a consequence of the WT prototype used, the WT loop $\mathbf{w}_m[n]\,|_{n\in W}$ is proportional to the VCG derivative and describes the velocity of evolution of the EHV in a time interval W. Assuming that the noise is spatially homogeneous, the direction with maximum projection of the WT in the region close to the wave boundary would define the ECG lead maximizing the local SNR, and thus, the most appropriate for boundary delineation. The main direction $\mathbf{u} = [u_{\mathrm{X}}, u_{\mathrm{Y}}, u_{\mathrm{Z}}]^T$ of EHV variations at a scale 2^m on any time interval W is given by the director vector of the best straight linear fit to all points in the WT loop $\mathbf{w}_m[n]$ [Fig. 2(d)]. By adequately choosing the time interval W, it is possible to find the $\mathbf{u}$ corresponding to the lead most suited for delineation purposes. It should be noted that the time intervals I (used for projecting) and W (used for linear fitting) can be different, depending on each wave's specificity.

The strategy proposed for ML boundary delineation using WT loops is based on a multistep iterative search for a *better* spatial lead for delineation improvement (with *steeper* slopes), particularized for each boundary. At each step (i), the vector $\mathbf{u}^{(i)}$ is determined *separately for each beat and boundary*, by adapting and updating the interval W, defined specifically for each wave and boundary, in a way to increase the SNR and ensure steep slopes in $w^{(i)}_{d,m}[n]$ obtained by (4). The goal is to construct a *derived wavelet* signal well suited for boundaries location, using the same detection criteria as in the SL delineator.[1]

[1] SL-threshold-based criteria were applied as reported in [2] except for T-wave end with $\xi_e(m) = 0.25 w_{x,m}[n_1^{(i)}]$.

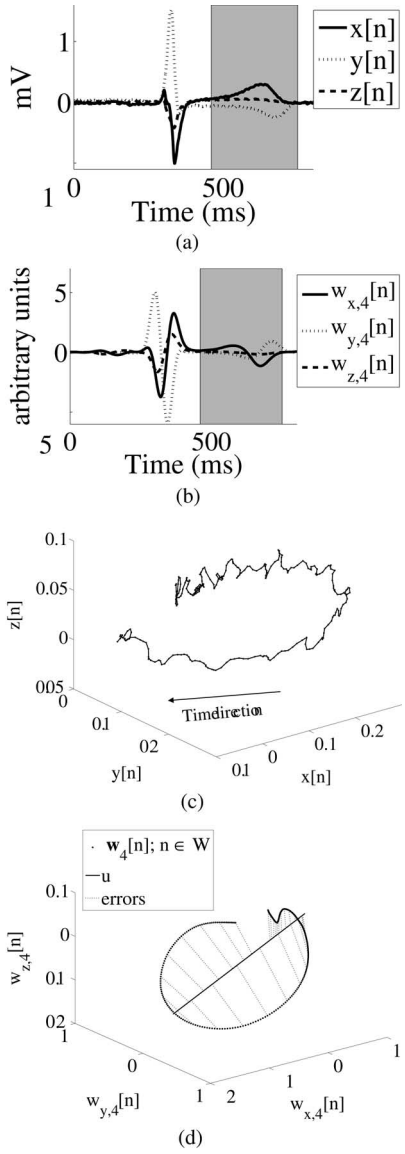

Fig. 2. Examples of ECG and the components of $\mathbf{w}_m[n]$ corresponding to whole beat in Frank leads ($n \in W$ for the gray area) and VCG loop and WT loop corresponding to the T wave ($n \in W$). (a) ECG leads. (b) WT at scale 2^4. (c) VCG loop of the T wave. (d) $\mathbf{w}_4[n]$ loop of the T wave, best line fit by TLS minimization to the entire loop and some fitting residues in TLS sense.

Considering the VCG loop $\mathbf{s}[n]$ in any time interval I, a *derived* lead $d[n]$ defined by the axis $\mathbf{u}$ can be constructed by projecting the points of the VCG loop

$$d[n] = \frac{\mathbf{s}^T[n]\mathbf{u}}{\|\mathbf{u}\|}, \qquad n \in I. \tag{3}$$

The variable $d[n]$ combines the information provided by the three leads in $\mathbf{s}[n]$. Instead, the WT loop ($\mathbf{w}_m[n]$) can be projected, and a *derived wavelet* signal $w_{d,m}[n]$, corresponding to the ECG lead defined by the axis $\mathbf{u}$, can be constructed as

$$w_{d,m}[n] = \frac{\mathbf{w}_m^T[n].\mathbf{u}}{\|\mathbf{u}\|}, \qquad n \in I. \tag{4}$$

1) General Algorithm for ML Boundary Location: For each beat and boundary, the following strategy is applied (particular details for each boundary are described in later sections).

INITIALIZATION

a_0) An initial search window adequate to find the EHV's main direction in the boundary is defined as $W^{(1)}$.

b_0) The initial main direction of EHV variations $\mathbf{u}^{(1)}$ is estimated using the adequate scale 2^m, as the best line fit in total least squares (TLS) sense [6] to $\mathbf{w}_m[n]\,|_{n \in W^{(1)}}$.

c_0) The loop $\mathbf{w}_m[n]\,|_{n \in [n_{\mathrm{QRS},k-1},\, n_{\mathrm{QRS},k+1}]}$, with $n_{\mathrm{QRS},k}$ being the median of SL-derived locations for the QRS complex in the kth beat, is projected over $\mathbf{u}^{(1)}$ to construct the new derived WT signal $w_{d,m}^{(1)}[n]$.

d_0) SL delineation over $w_{d,m}^{(1)}[n]$ allows to locate $n_o^{(1)}$ or $n_e^{(1)}$, the boundary position at step 1.

ITERATION—STEP (i)

a) The search window $W^{(i)}$ is updated while attending to the boundary location provided by the previous step $(i-1)$.

b) The main direction of EHV variations $\mathbf{u}^{(\mathbf{i})}$ is estimated as the TLS best line fit to $\mathbf{w}_m[n]$, $n \in W^{(i)}$.

c) The new derived WT signal $w_{d,m}^{(i)}[n]$ is constructed by projecting the loop $\mathbf{w}_m[n]\,|_{n \in [n_{\mathrm{QRS},k-1},\, n_{\mathrm{QRS},k+1}]}$.

d) IF $w_{d,m}^{(i)}[n]$ is less fitted for boundary location than $w_{d,m}^{(i-1)}[n]$, OR no significant maximum of $w_{d,m}^{(i)}[n]$ was found THEN $n_o^{(i-1)}$ or $n_e^{(i-1)}$ (found in the previous step) is adopted as ML mark; STOP; ELSE SL delineation of the boundary is performed over $w_{d,m}^{(i)}[n]$ to find $n_o^{(i)}$ or $n_e^{(i)}$ updated marks.

e) IF no relevant change is found in the boundary location THEN $n_o^{(i)}$ or $n_e^{(i)}$ is adopted as ML mark; STOP; ELSE REPEAT from a).

In the traditional least-squares criteria, it is assumed that errors occur in only one *observed* variable, while the other variables are exactly known. However, all the three signals used to define the WT loop of (2) are representations of observed ECG leads that can contain noise contamination. The TLS fitting does not assume that some variables are error-free and minimizes the distance between each observation and the fitted line (orthogonal deviations are considered [6]), as illustrated in Fig. 2(d). It must be also remarked that the use of WT loop to base the lead direction instead of taking directly the VCG loop is relevant, as it allows to avoid the high- and low-frequency noise contamination, and thus, produces a more accurate lead selection for delineation [Fig. 2(c) and (d)]. In addition, if the Frank leads were not recorded:

1) Frank leads can also be synthesized from the standard 12-lead system [7];
2) the ML delineation methodology can be applied over any set of three ECG orthogonal leads;
3) considering WT loops in a 2-D plane instead of in a 3-D space is also possible, thus allowing to apply this methodology to any two ECG orthogonal leads.

In cases of extreme noise or with very poor signal amplitude, the lead search can fail in finding the optimal projection, giving

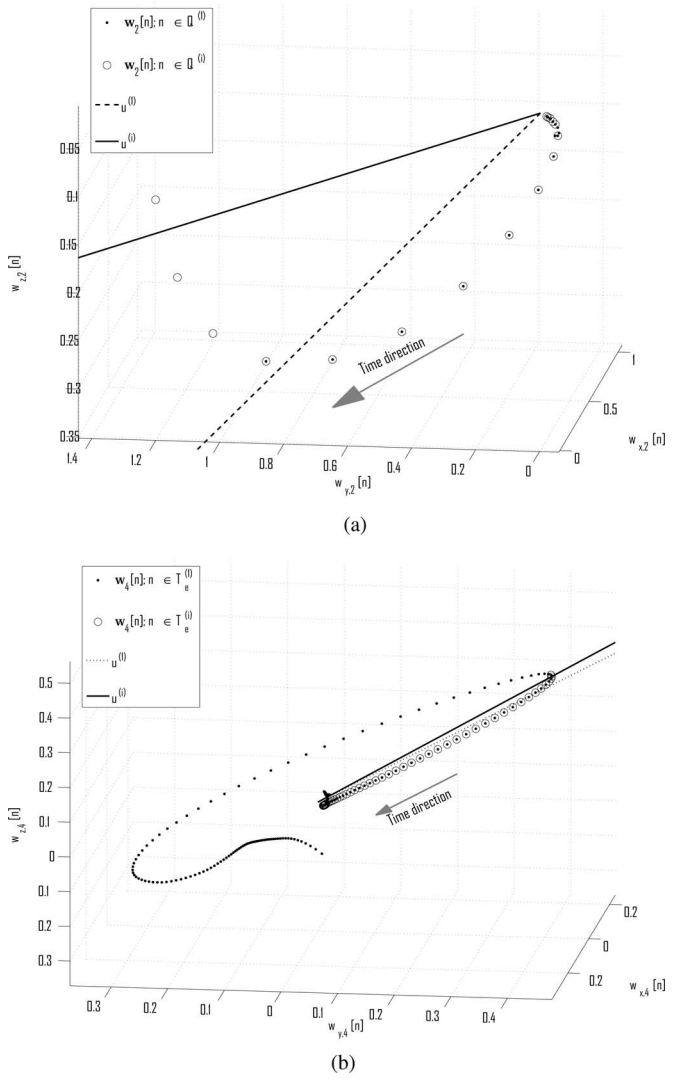

Fig. 3. Example of ML delineation (files from CSEDB database [9]): WT loops and the direction of the best line fit at the initial and final step ($i = 2$). (a) ML QRS onset location. (b) ML T end location.

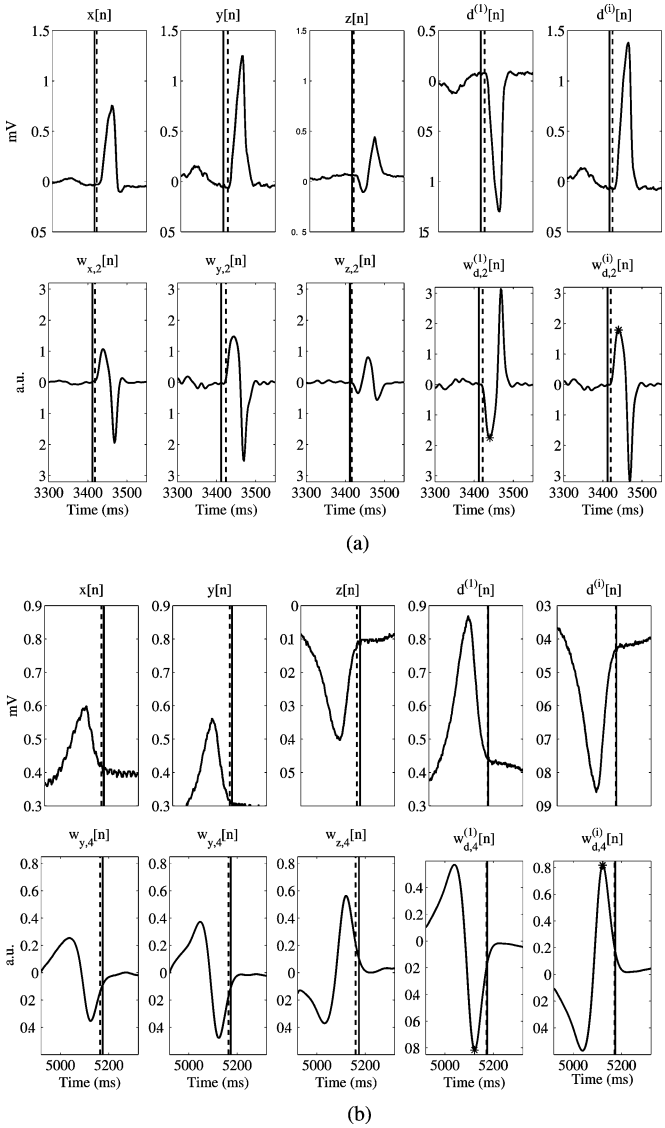

Fig. 4. Comparison between SL and ML delineation: ECG in orthogonal leads $x[n]$, $y[n]$, $z[n]$, the corresponding WT signals $w_{x,m}[n]$, $w_{y,m}[n]$, $w_{z,m}[n]$, the derived ECG signals $d^{(1)}[n]$, $d^{(i)}[n]$, and WT signals $w^{(1)}_{d,m}[n]$, $w^{(i)}_{d,m}[n]$, following the directions of vectors $\mathbf{u}^{(1)}$ and $\mathbf{u}^{(i)}$ found for the kth beat (Fig. 3), respectively, for QRS onset and T-wave end. Vertical dashed lines stands for the mark found in the respective lead, solid line stands for *median referee* marks, and the stars stands for the first (last) significant maximum modulus in the constructed lead. (a) QRS onset delineation ($m = 2$, n is an arbitrary neighborhood of the QRS complex for the kth beat), $i = 2$. (b) T end delineation ($m = 4$, $n \in Tw_{[1]}$, $i = 2$).

inconsistent boundaries (e.g., an onset after the wave peak). These boundaries were discarded.

2) Specific Parameters for QRS Complex Boundaries: ML location of the QRS boundaries is performed using the WT loop at scale 2^2, as illustrated for QRS onset in Figs. 3(a) and 4(a). Let us define $n^{(0)}_{\mathrm{QRS},o}(n^{(0)}_{\mathrm{QRS},e})$ as the earliest (latest) QRS onset (end) location given by the SL methods (over each orthogonal lead) and $n^{(0)}_{\mathrm{QRS},f}$ $(n^{(0)}_{\mathrm{QRS},l})$ is the earliest (latest) significant maximum modulus location. The initial search window for QRS onset and end is taken as

$$W^{(1)} = \mathrm{Q}^{(1)} = \left[n^{(0)}_{\mathrm{QRS},o} - 4s_{\mathrm{CSE}(\mathrm{QRS_{on}})},\ n^{(0)}_{\mathrm{QRS},f}\right] \quad (5)$$

$$W^{(1)} = \mathrm{S}^{(1)} = \left[n^{(0)}_{\mathrm{QRS},l}\ ,\ n^{(0)}_{\mathrm{QRS,e}} + 4s_{\mathrm{CSE}(\mathrm{QRS_{end}})}\right] \quad (6)$$

respectively, where $s_{\mathrm{CSE}(\mathrm{QRS_{on}})} = 3.25$ ms and $s_{\mathrm{CSE}(\mathrm{QRS_{end}})} = 5.8$ ms are the standard deviation tolerance values provided in [8]. At each iteration (i), the search window is updated

$$W^{(i)} = \mathrm{Q}^{(i)} = \left[n^{(i-1)}_{\mathrm{QRS},o} - 4s_{\mathrm{CSE}(\mathrm{QRS_{on}})},\ n^{(i-1)}_{\mathrm{QRS},f}\right] \quad (7)$$

$$W^{(i)} = \mathrm{S}^{(i)} = \left[n^{(i-1)}_{\mathrm{QRS},l}\ ,\ n^{(i-1)}_{\mathrm{QRS},e} + 4s_{\mathrm{CSE}(\mathrm{QRS_{end}})}\right] \quad (8)$$

where $n^{(i-1)}_{\mathrm{QRS},o}$ $(n^{(i-1)}_{\mathrm{QRS},e})$ is the QRS onset (end) position found at step $(i-1)$ and $n^{(i-1)}_{\mathrm{QRS},f}$ $(n^{(i-1)}_{\mathrm{QRS},l})$ is the location of the first (last) significant maximum modulus of $w^{(i-1)}_{d,m}[n]$.

IF $n^{(i)}_{\mathrm{QRS,f}}$ $(n^{(i)}_{\mathrm{QRS},l})$ has the same polarity as $n^{(i-1)}_{\mathrm{QRS},f}$ $(n^{(i-1)}_{\mathrm{QRS},l})$, equal or lower amplitude, and QRS complex morphology

includes a Q (S) wave, it is considered that the lead constructed at step (i) is not better for QRS onset (end) location than that constructed at step $(i-1)$ and the iteration STOP criterion of d) is applied. The iteration STOP criterion of e) is applied if the the same location is achieved for three iterations.

3) Specific Parameters for T-Wave Boundaries: ML delineation of T-wave boundaries is illustrated for the T end in Figs. 3(b) and 4(b). Scale $2^m = 2^5$ is considered if in the SL delineation, the scale 2^5 was used for T-wave detection for at least two out of the three leads, and $m = 4$ otherwise [2]. The T-wave morphology is typically more simple; thus, a single initial search window $W^{(1)} = \mathrm{T}_o^{(1)} = \mathrm{T}_e^{(1)}$, taken as the union of the SL search windows on the orthogonal leads, is considered for each beat, both regarding the wave's onset and end. The search window for *T onset* at iteration (i) is updated as

$$W^{(i)} = \mathrm{T}_o^{(i)} = \left[n_{\mathrm{T},o}^{(i-1)} - 4s_{\mathrm{CSE}}(\mathrm{T_{on}});\ n_{\mathrm{T},f}^{(i-1)}\right]$$

and the search window for *T end* is actualized as

$$W^{(i)} = \mathrm{T}_e^{(i)} = \left[n_{\mathrm{T},l}^{(i-1)};\ n_{\mathrm{T},e}^{(i-1)} + 4s_{\mathrm{CSE}}(\mathrm{T_{end}})\right]$$

where $n_{\mathrm{T},o}^{(i-1)}(n_{\mathrm{T},e}^{(i-1)})$ is the T onset (end) position, according to iteration $(i-1)$, $n_{\mathrm{T},f}^{(i-1)}(n_{\mathrm{T},l}^{(i-1)})$ is the location of the first (last) significant maximum modulus, associated with the T wave in $w_{d,m}^{(i-1)}[n]$, and $s_{\mathrm{CSE}(\mathrm{T_{on}})} = s_{\mathrm{CSE}(\mathrm{T_{end}})} = 15.3$ ms is the tolerance value given in [8] for T-wave end (no tolerance value for T-wave onset was given).

If $n_{\mathrm{T},f}^{(i)}(n_{\mathrm{T},l}^{(i)})$ has equal or lower amplitude than $n_{\mathrm{T},f}^{(i-1)}(n_{\mathrm{T},l}^{(i-1)})$, it is considered that the lead constructed at step (i) is not better for T onset (end) location than that constructed at step $(i-1)$, and applied the iteration STOP criterion of item d). The iteration STOP criterion e) is applied if the locations in two consecutive steps differ by less than two samples.

D. Validation

The evaluation of the automatic delineation strategies was performed over real files from the available manually annotated ECG databases (as the true onsets and end on clinical ECG signals are unknown). Two standard databases have been repeatedly used for evaluation of ECG delineation systems: the Common Standards for Electrocardiography ML measurement database (CSEDB [9], 42 short signals in 15 leads at 500 Hz) and the QT database (QTDB [10], 105 files, 15 min long, in two leads at 250 Hz). In CSEDB, manual annotations were made by five cardiologists having in view all the available leads (ML-based); for a beat per file are provided *median referee* annotations after an elaborated reviewing scheme of four rounds with outlier rejection, designed to reduce intra- and interobserver variability. QTDB included annotations from two cardiologists, but only the first referee is considered here, who provided marks for at least 30 beats per file (in a total of more than 3600 annotated beats). More recently, the Physikalisch-Technische Bundesanstalt (PTB) database (PTBDB, 549 files at 1000 Hz) has also been manually annotated in the context of the "PhysioNet/computers in cardiology challenge 2006: QT interval measurement" competition [11]. A set of reference annotations (one beat per file) was published in [12], consisting of SL manual annotations for QRS onset and T-wave end (based on lead II), done by four cardiologists and one biomedical engineer, and a *median referee* annotation (after outlier rejection). According to [12], in more than 15% of the records in PTBDB, no T wave could be definitely recognized in lead II, and, in such a case, the referees were instructed to mark the T-wave end as a group at one of the leads where the T wave was better manifested.

The delineation system was validated over these three databases by comparing the automatic marks found with the provided referee marks. It should be remarked that not all beats are annotated, nor all waves and boundaries are given for each annotated beat. In CSEDB, a total of 42 beats are partially annotated, including 32 complex QRS onsets, and 26 ends and 27 T-wave ends, with no T onsets. In QTDB, more than 3600 annotated beats are provided; nevertheless, given marks also vary from beat to beat. In PTBDB, only the QRS onset and T-wave end are available, in one beat per file, and, in six of those, the first beat, which is not reliable for WT methods due to border effect, is annotated; thus, only 542 beats can be considered.

In CSEDB and PTBDB databases, three different VCG systems were considered: *lead set F*—defined by recorded orthogonal Frank leads (X,Y,Z); *lead set M*—defined by leads *V5*, *aVF*, and *V2*, a subset of three mutually orthogonal leads out of the standard 12-lead system; *lead set D*—defined by the synthesized orthogonal leads (X,Y,Z) from the 12-lead system, by using the coefficients provided by the inverse *Dower matrix* [7]. These VCG systems were chosen because they are defined by well-known leads, which are likely to be familiar to clinicians, but any other combination of three orthogonal leads could be used instead, and other transformations from 12 to 3 leads rather than Dower matrix can be considered. The ML over the systems F, M, and D was compared with SL delineation over each of the 15 recorded leads. Additionally, SL followed by the post-processing decision rules (SLR) described in Section II-B was applied over 12 leads, and also over the 3 leads in each lead set (F, M, and D), but with $\mathsf{k} = 0$ (no protection rules at all).

Since QTDB includes only two leads, ML was applied using loops in the 2-D plane instead of in the 3-D space. Regarding the orthogonality of the available leads, the QTDB was divided into four subgroups: *QTDB1* —7 records with orthogonal leads from the 12-lead standard system, in which the ML delineation can be applied directly using a 2-D approach; *QTDB2*—57 records with no identified leads, here assumed to be orthogonal and treated as the ones in *QTDB1*; *QTDB3*—34 records with no orthogonal and no parallel leads, which were orthogonalized by constructing a new ECG lead orthogonal to one of the provided leads; *QTDB4*—7 records with parallel leads, which cannot be orthogonalized, and therefore, will not be considered for the validation (leads *I* and *V5* from the 12-lead standard system). Additionally, a combined mark was obtained by choosing for each fiducial point the location on the lead with less error (best mark). Although this last approach cannot be considered as a rule to apply in real practice where no reference marks exist, it is a reasonable way to compare the two SL annotation sets with the manual annotations that have been performed having in view all available leads.

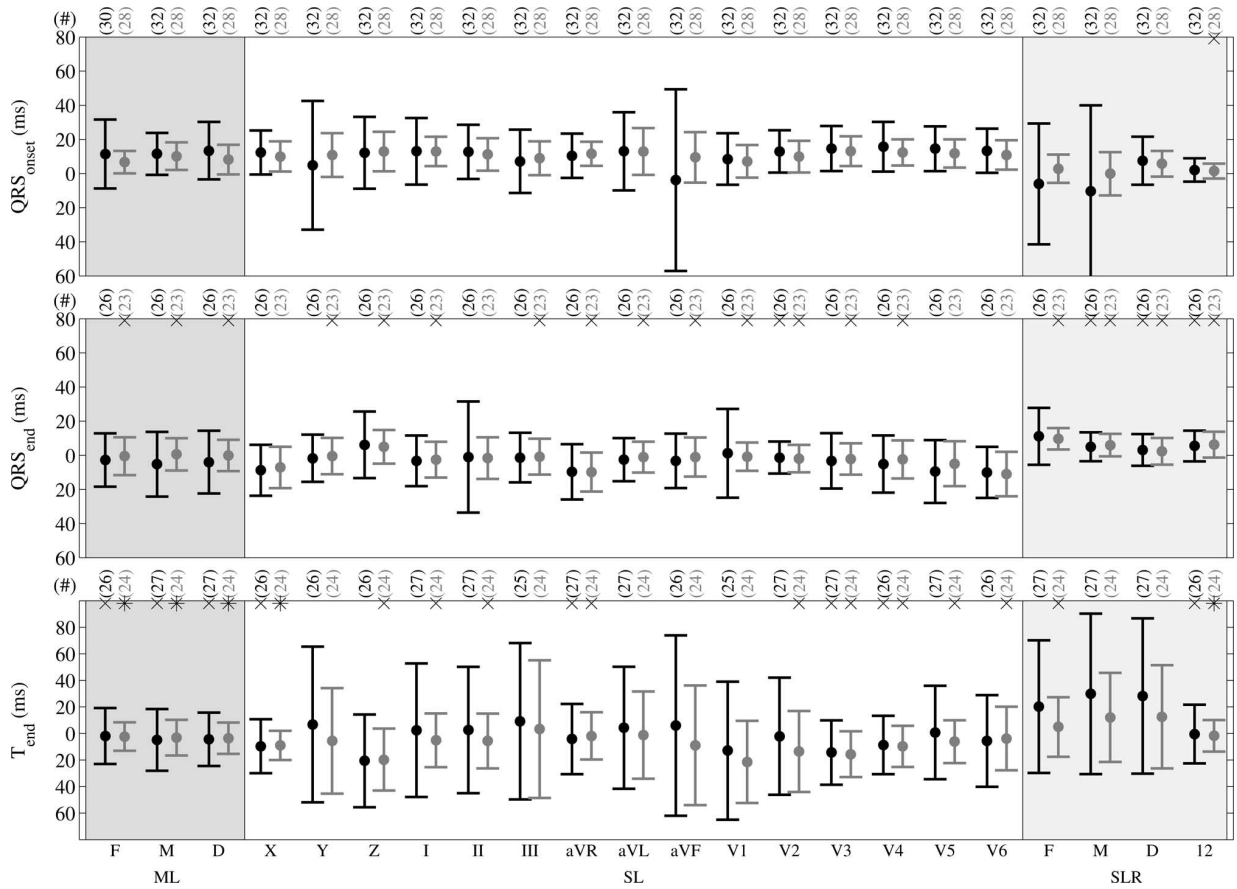

Fig. 5. Delineation results in CSEDB: comparison between ML over lead subsets F, M, and D (darker gray area), SL over each of the 15 available leads, and SLR over the standard 12 leads and over the three orthogonal leads in F, M, and D (lighter gray area). The symbol # denotes the number of TP out of 32 reference marks provided (black) or after excluding extreme cases in each approach (gray); results fulfilling loose criterion are marked with $\times$ and fulfilling strict criterion are marked with a star.

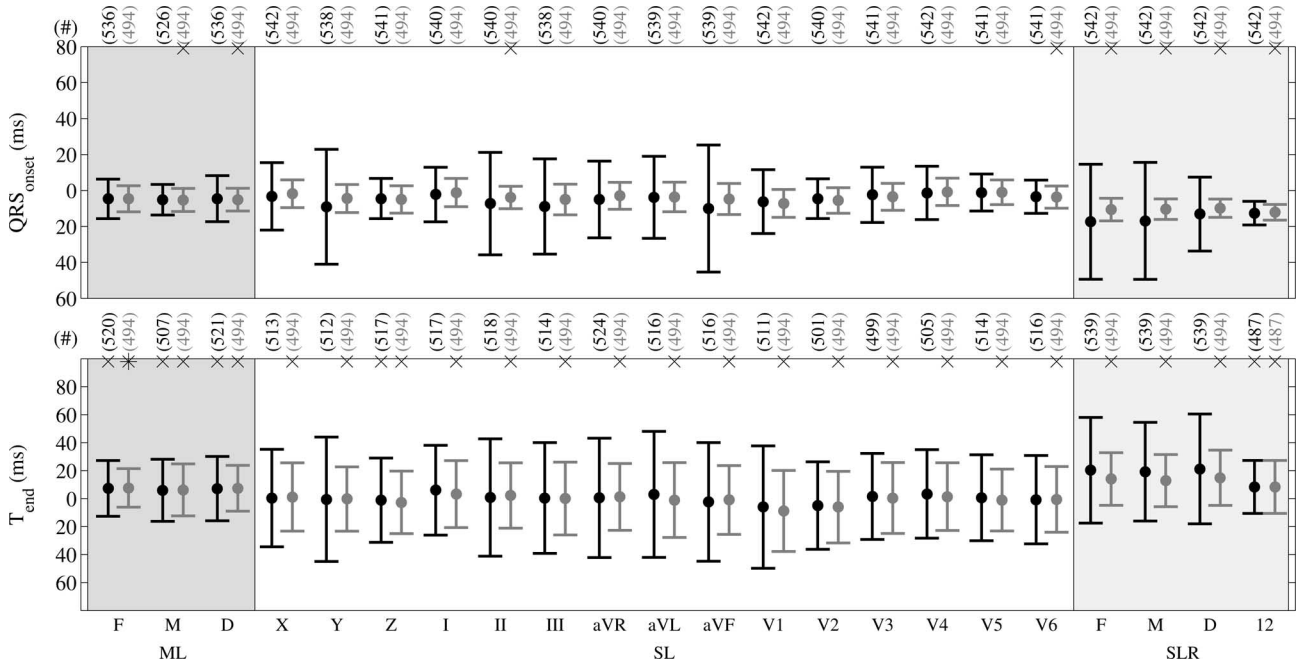

Fig. 6. Delineation results in PTBDB: comparison between ML over lead subsets F, M and D (darker gray area), SL over each of the 15 available leads, and SLR over the standard 12 leads and over the three orthogonal leads in F, M, and D (lighter gray area). The symbol # denotes the number of TP out of 542 reference marks provided (black) or after excluding extreme cases in each approach (gray); results fulfilling loose criterion are marked with $\times$ and those fulfilling strict criterion are marked with a star.

The *detection* performance was evaluated by calculating the *sensitivity* $S = 100\,\mathrm{TP}/(\mathrm{TP}+\mathrm{FN})$, where TP is the number of true positive detections and FN stands for the number of false negative detections. For the CSEDB, S was not calculated given the low number of annotated beats. The delineation error (ε) was taken as the *automatically detected boundary minus the respective referee mark*, and in each database, the mean (m_ε) and standard deviation (s_ε) of ε were evaluated across files, considering all TP detections. Additionally, for CSEDB and PTBDB, the aforementioned parameters were also calculated after the exclusion of the 10% most *extreme cases*, which are likely to be outliers. Concerning QTDB, since several beats are annotated per file, the standard deviation of the error ε was first calculated across beats for each file and then averaged across record. Thus, for this database, $\bar{s}_\varepsilon$ stands for the mean standard deviation across files.

According to the recommendations in [8], *the standard deviation of the differences from the reference should not exceed certain limits*. These values $(2s_{\mathrm{CSE}})$ correspond to two standard deviations of the differences between the median of the individual readers manual annotations used for constructing CSEDB and were already referred to in this paper as they were used to define search windows in the ML delineation system (Section II-C). In spite of being widely accepted as a way for defining a tolerance for the automatic marks errors dispersion, it is not consensual if an algorithm should accomplish the following.

1) Loose criterion: $s < 2s_{\mathrm{CSE}}$ [5], [13]–[15].
2) Strict criterion: $s < s_{\mathrm{CSE}}$ [16], [17].

III. Results

ML approach was applied to each of the three different VCG systems considered (F, M, and D). SL delineation was performed over each of the 15 recorded leads and SL followed by the postprocessing decision rules (SLR) was applied over 12 leads, and also over the three leads in each lead set (F, M, and D). In Figs. 5 and 6, m_ε and s_ε in CSEDB and PTBDB, respectively, are plotted, both considering all true positive detections and after excluding the extreme cases. As expected, results from SL denote a high dependency on the specific lead considered. From the strategies based on multiple leads, the SLR over 12 leads is the one that achieves the best performance, especially for QRS boundaries, but with lower sensitivity for T end in PTBDB. SLR over three leads presents a high error dispersion both for QRS complex onset and T-wave end. ML delineation over three orthogonal leads achieved in all datasets better results than most isolated leads, though slightly worse than the best SL result. In most cases, it presented a reduced error dispersion compared to SLR over three leads. In particular, ML over lead set F outperformed any SL-based delineation for T-end delineation.

For the sake of comparison, other published results also validated in CSEDB can be found in Table I. Note that the results reported in [5] and [16] used the described decision rules over the 15 sets of marks, while no information was provided in [13] about which ML rules were used.

Two typical situations for QRS onset delineation are illustrated in Fig. 7. In Fig. 7(a) is presented a case in which the ML methodology fails, as two out of the three orthogonal leads showed lower errors than the ML approach. This is due to an initial positive wave in the QRS that is not detected in the last step of the iterative method, resulting from a less suited lead direction. This type of errors is, however, not systematic in the presence of small Q/R waves. As a matter of fact, in Fig. 7(b), one can

TABLE I
Other Published Delineation Systems With Selection Rules Validated Over CSEDB

	[5]	[16]	[13]
QRS onset			
(#/32)	(30)	(32)	(NR)
$m_\varepsilon \pm s_\varepsilon$	-2.1 ± 7.4	0.9 ± 3.6 ×	$NR \pm 2.0$ *
QRS end			
(#/27)	(25)	27	(NR)
$m_\varepsilon \pm s_\varepsilon$	-0.2 ± 3.6×	-0.6 ± 7.1	$NR \pm 4.0$ ×
T end			
(#/27)	(26)	NA	(NR)
$m_\varepsilon \pm s_\varepsilon$	2.6 ± 10.5*	NA	NR±20.0 ×

NR: not reported; NA: not applicable. Results fulfilling loose criterion are marked with symbol × and strict criterion with symbol *.

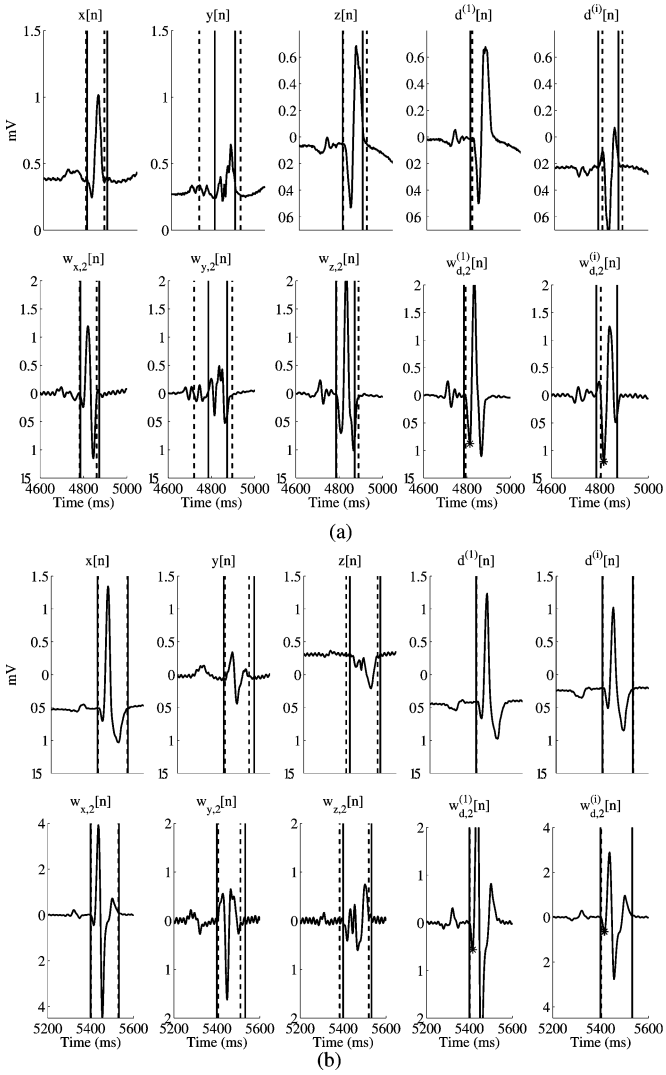

Fig. 7. Comparison between SL and ML delineation in the case of small initial waves. (a) Example in which the ML fails ($i = 2$). (b) Case in which ML performs correctly ($i = 3$). Notation used is the same as in Fig. 4(a).

TABLE II
QRS BOUNDARIES DELINEATION RESULTS IN QTDB. (a) QRS COMPLEX ONSET. (b) QRS COMPLEX END

(a)

		ML	lead 1 SL	lead 2 SL	best mark
QTDB 1 (7 files)	# beats / 312	293	312	312	312
	$Se(\%)$	94	100	100	100
	$m_\varepsilon \pm \bar{s}_\varepsilon$, ms	6.4 ± 10.6	4.7 ± 10.8	12.3 ± 11.5	5.3 ± 8.7
QTDB 2 (57 files)	# beats / 1908	1885	1907	1906	1907
	$Se(\%)$	99	100	100	100
	$m_\varepsilon \pm \bar{s}_\varepsilon$, ms	5.9 ± 11.3	5.5 ± 10.5	6.6 ± 11.2	4.5 ± 7.8
QTDB 3 (34 files)	# beats / 1192	1132	1179	1188	1192
	$Se(\%)$	95	99	100	100
	$m_\varepsilon \pm \bar{s}_\varepsilon$, ms	10.4 ± 11.3	11 ± 14.7	9.3 ± 10.8	8.6 ± 8.6
all (98 files)	# beats / 3412	3310	3398	3406	3411
	$Se(\%)$	97	100	100	100
	$m_\varepsilon \pm \bar{s}_\varepsilon$, ms	7.5 ± 11.2	7.3 ± 12	7.9 ± 11.1	6 ± 8.2

(b)

		ML	lead 1 SL	lead 2 SL	best mark
QTDB 1 (7 files)	# beats / 312	312	312	312	312
	$Se(\%)$	100	100	100	100
	$m_\varepsilon \pm \bar{s}_\varepsilon$, ms	2 ± 21.2	-6.2 ± 13.2	-0.1 ± 13	3.3 ± 11 ×
QTDB 2 (57 files)	# beats / 1908	1902	1907	1906	1907
	$Se(\%)$	100	100	100	100
	$m_\varepsilon \pm \bar{s}_\varepsilon$, ms	3.3 ± 11.7	-1 ± 10.9 ×	2.4 ± 13.1	0.6 ± 8.4 ×
QTDB 3 (34 files)	# beats / 1192	1157	1179	1188	1192
	$Se(\%)$	97	99	100	100
	$m_\varepsilon \pm \bar{s}_\varepsilon$, ms	11.6 ± 11.6	9.4 ± 11.5 ×	11.1 ± 12.1	6.4 ± 8.7 ×
all (98 files)	# beats / 3412	3371	3398	3406	3411
	$Se(\%)$	99	100	100	100
	$m_\varepsilon \pm \bar{s}_\varepsilon$, ms	6.1 ± 12.3	2.2 ± 11.3 ×	5.2 ± 12.7	2.8 ± 8.7 ×

Results fulfilling loose criterion are marked with symbol ×.

TABLE III
T-WAVE BOUNDARIES DELINEATION RESULTS IN QTDB. (a) T-WAVE ONSET. (b) T-WAVE END

(a)

		ML	lead 1 SL	lead 2 SL	best mark
QTDB 1 (2 files)	# beats / # total beats	45/46	44/46	46/46	46/46
	$Se(\%)$	98	96	100	100
	$m_\varepsilon \pm \bar{s}_\varepsilon$, ms	13.3 ± 22.5 ×	8.6 ± 25.2 ×	14.1 ± 22.5 ×	11.9 ± 19.6 ×
QTDB 2 (33 files)	# beats / # total beats	766/958	799/958	808/958	869/958
	$Se(\%)$	80	83	84	91
	$m_\varepsilon \pm \bar{s}_\varepsilon$, ms	18 ± 28.9 ×	25.5 ± 36.1	14 ± 32.8	10.4 ± 28.2 ×
QTDB 3 (10 files)	# beats / # total beats	281/298	279/298	292/298	296/298
	$Se(\%)$	94	94	98	99
	$m_\varepsilon \pm \bar{s}_\varepsilon$, ms	22 ± 24.7 ×	20.2 ± 28.7 ×	0 ± 28.7 ×	16.1 ± 23.8 ×
all (45 files)	# beats / # total beats	1092/1302	1122/1302	1146/1302	1211/1302
	$Se(\%)$	84	86	88	93
	$m_\varepsilon \pm \bar{s}_\varepsilon$, ms	18.7 ± 27.6 ×	23.6 ± 33.9 ×	0 ± 31.4 ×	11.7 ± 26.8 ×

(b)

		ML	lead 1 SL	lead 2 SL	best mark
QTDB 1 (7 files)	# beats / # total beats	307/312	311/312	312/312	312/312
	$Se(\%)$	98	100	100	100
	$m_\varepsilon \pm \bar{s}_\varepsilon$, ms	-8.1 ± 24.6 ×	-18.1 ± 28.5 ×	3.7 ± 37.6	-12.2 ± 17.8 ×
QTDB 2 (55 files)	# beats / # total beats	1760/1827	1798/1827	1789/1827	1819/1827
	$Se(\%)$	96	98	98	100
	$m_\varepsilon \pm \bar{s}_\varepsilon$, ms	11.4 ± 24 ×	3.1 ± 26.9 ×	0.3 ± 26.8 ×	1.7 ± 20.1 ×
QTDB 3 (34 files)	# beats / # total beats	1153/1192	1156/1192	1179/1192	1192/1192
	$Se(\%)$	97	97	99	100
	$m_\varepsilon \pm \bar{s}_\varepsilon$, ms	5.5 ± 17.4 ×	-6 ± 28 ×	-0.2 ± 21.2 ×	-0.4 ± 16.9 ×
all (96 files)	# beats / # total beats	3220/3331	3265/3331	3280/3331	3323/3331
	$Se(\%)$ - $P^{+}_{min}(\%)$	97-98	98-98	98-98	100-98
	$m_\varepsilon \pm \bar{s}_\varepsilon$, ms	7.9 ± 21.7 ×	-1.7 ± 27.4 ×	0.4 ± 25.6 ×	0 ± 18.8 ×

Results fulfilling loose criterion are marked with symbol ×.

find a similar case in which the ML achieves an improvement in the delineation, in spite of the noise contamination.

In Tables II and III are presented the values of S and m_ε, $\bar{s}_\varepsilon$ in each QTDB subgroup, and the global results (all). It was found that a relative low number of extreme cases were causing a large fraction of the global error. The exclusion of the 10% more extreme files in each approach allowed a generalized improvement in the errors dispersion, with bias increase in some cases.

IV. DISCUSSION

Globally, ML allowed an error dispersion similar to that obtained using SLR over the 12 leads, including other published approaches (Table I). High sensitivity values were

found, resulting from the fact that only a very low number of boundaries were considered to be inconsistent and discarded.

The automatic procedures are marking the QRS onset on CSEDB files later than the referees, as can be seen from the *positive bias* found in most of the cases. This is likely to be due to situations as the ones illustrated in Fig. 7(a). With respect to the PTBDB files, it is known that the manual QRS onset (all) and T end (85%) reference marks are SL-based in lead II [12]. This is reflected in the lowest bias found for SL over lead II in T-wave end location. Either ML or SLR when compared with SL-based reference marks (PTBDB) show a negative bias for QRS onset and a positive bias for T-wave end. Clearly, this is in accordance with the strategy of using information from multiple leads in order to locate the earliest and the latest signs of ventricular activity.

The ML over the VCG was able to provide, from only three ECG leads, boundary locations as stable as the ones provided by other methods using many more leads. It should be remarked that the proposed method requires the WT calculation of three leads, with delineation procedures involving a variable number of signals. Thus, even by considering fitting and projecting features, the ML strategy is usually more efficient than applying SL to 12 leads, as the number of steps needed is not very high. The number of iterations was low, with mean values between three and four iterations for QRS boundaries and less than two for T boundaries. Thus, the results presented denote a clear performance improvement.

Among the VCG systems considered, *lead set* F *achieved the best global performance*. This is in accordance with the results of the "PhysioNet/computers in cardiology challenge 2006: QT interval measurement," in which the QT interval in a representative beat per file was evaluated over the PTBDB files [4], [11], [18].

With respect to ML delineation using only two leads (QTDB files), global results are similar to the worse SL result for QRS boundaries, thus outperforming the best SL result for T-wave boundaries. Using a 2-D approach over two orthogonal leads seems insufficient for QRS boundaries. The ML delineation of the T wave in files with two orthogonal (or orthogonalized) leads is more stable than using any of the two leads by themselves. Further studies should be carried out to fully evaluate the performance using only two leads.

The methods were validated over the available ML databases with reference annotations, among which only the CSEDB can be considered to have truly ML-based annotations, with the referee considering all leads during the annotation process. In addition to the fact that CSEDB includes just a very limited number of beats, the referees typically tend to base the mark in a dominant clear lead, instead of using combination of them. To have a fairer evaluation of the proposed methods, truly ML manual annotations should be obtained, for instance, by presenting the VCG loop to the referee. These kinds of annotations, which are not available today, will be better matched to the physiological boundary and would allow a better quantification of the true improvement achieved by the proposed ML methods.

V. Conclusion

A novel ML WT-based strategy for ECG boundaries delineation was proposed here and evaluated with respect to the QRS and T-wave boundaries. Using different leads is crucial to locate the global waves boundaries, which can be imperceptible in a particular lead. The automatic proposed ML approach allows to deal with multiple leads, taking advantage of their availability to further improve the delineation, by constructing a WT signal more fitted for the specific boundary location. The ML system provided more robust and more accurate boundaries locations than any electrocardiographic lead by itself and outperformed strategies based on rule selection after SL delineation.

Among VCG systems, the lead set F (directly recorded Frank leads) achieved the best global performance. The results also showed that ML delineation with two orthogonal (or orthogonalized) leads, especially for the T wave, outperforms both SL results, and thus, is better than any possible selection rule for T end delineation. Furthermore, the ML delineation strategies developed are general and can be applied to any orthogonal lead set; the VCG systems considered here were chosen because they are defined by well-known leads, which are likely to be familiar to clinicians; however, any other combination of three orthogonal leads (real or derived) could be used instead. In particular, this method has also been partially validated over the first three principal components, outperforming the results using inverse Dower transformation [19]. Note that techniques based on principal or independent components analysis have been widely used, both for filtering and segmentation of ECG signals [20]–[22].

As far as we know, this is the first delineation system that explicitly constructs a new better suited ECG lead for that purpose, instead of locating the fiducial points in one available lead. This solves the problem of different latencies on the waves' onsets and ends found in different leads and combine the information provided by the multiple leads, taking advantage of their spacial dependency, and giving a unique annotation for the onset and end of the cardiac electric phenomena. Globally, results within the tolerance bounds were obtained for all boundaries, showing that the proposed methods are quite robust against noise and morphological variations.

References

[1] C. Li, C. Zheng, and C. Tai, "Detection of ECG characteristic points using wavelet transforms," *IEEE Trans. Biomed. Eng.*, vol. 42, no. 1, pp. 21–28, Jan. 1995.

[2] J. P. Martínez, R. Almeida, S. Olmos, A. P. Rocha, and P. Laguna, "Wavelet-based ECG delineator: Evaluation on standard databases," *IEEE Trans. Biomed. Eng.*, vol. 51, no. 4, pp. 570–581, Apr. 2004.

[3] J. Malmivuo and R. Plonsey. (1995). *Bioelectromagnetism—Principles and Applications of Bioelectric and Biomagnetic Fields*. London, U.K.: Oxford Univ. Press [Online]. Available: http://butler.cc.tut.fi/malmivuo/bem/bembook/index.htm (accessed Dec. 2006).

[4] R. Almeida, J. P. Martínez, A. P. Rocha, P. Laguna, and S. Olmos, "Automatic multilead VCG based approach for QT interval measurement," in *Proc. Comput. Cardiol. Conf. 2006*, vol. 33, pp. 369–372.

[5] P. Laguna, R. Jané, and P. Caminal, "Automatic detection of wave boundaries in multilead ECG signals: Validation with the CSE database," *Comput. Biomed. Res.*, vol. 27, no. 1, pp. 45–60, Feb. 1994.

[6] S. Van Huffel and J. Vandewalle, *The Total Least Squares Problem: Computational Aspects and Analysis* (Frontiers in Applied Mathematics), vol. 9. Philadelphia, PA: SIAM, 1991.

[7] G. E. Dower, "The ECGD: A derivation of the ECG from VCG leads," *J. Electrocardiol.*, vol. 17, no. 2, pp. 189–191, 1984.
[8] The CSE Working Party, "Recommendations for measurement standards in quantitative electrocardiography," *Eur. J. Heart*, vol. 6, pp. 815–825, 1985.
[9] J. L. Willems, P. Arnaud, J. H. van Bemmel, P. J. Bourdillon, R. Degani, B. Denis, I. Graham, F. M. Harms, P. W. Macfarlane, and G. Mazzocca *et al.*, "A reference data base for multilead electrocardiographic computer measurement programs," *J. Amer. Coll. Cardiol.*, vol. 10, no. 6, pp. 1313–1321, 1987.
[10] P. Laguna, R. G. Mark, A. Goldberger, and G. B. Moody, "A database for evaluation of algorithms for measurement of QT and other waveform intervals in the ECG," in *Proc. Comput. Cardiol. 1997*, pp. 673–676.
[11] G. B. Moody, H. Koch, and U. Steinhoff, "The physionet computers in cardiology challenge 2006: QT interval measurement," in *Proc. Comput. Cardiol. Conf. 2006*, vol. 33, pp. 313–316.
[12] I. Christov, I. Otsinsky, I. Simova, R. Prokopova, E. Trendafilova, and S. Naydenov, "Dataset of manually measured QT intervals in the electrocardiogram," *Biomed. Eng. Online*, vol. 31, no. 5, pp. 5–31, 2006.
[13] J. S. Sahambi, S. N. Tandon, and R. K. P. Bhatt, "Using wavelet transform for ECG characterization," *IEEE Eng. Med. Biol. Mag.*, vol. 16, no. 1, pp. 77–83, Jan. 1997.
[14] H. J. L. M. Vullings, M. H. G. Verhaegen, and H. B. Verbruggen, "Automated ECG segmentation with dynamic time warping," in *Proc. 20th Ann. Int. Conf. IEEE Eng. Med. Biol. Soc.* Hong Kong: IEEE, 1998, pp. 163–166.
[15] J. A. Vila, Y. Gang, J. M. Presedo, M. Fernandez-Delgado, and M. Malik, "A new approach for TU complex characterization," *IEEE Trans. Biomed. Eng.*, vol. 47, no. 6, pp. 764–772, Jun. 2000.
[16] P. de Chazal and B. Celler, "Automatic measurement of the QRS onset and offset in individual ECG leads," in *Proc. 18th Ann. Int. Conf. IEEE Eng. Med. Biol. Soc.*, Amsterdam, The Netherlands: IEEE, 1996, pp. 1399–1400.
[17] P. Strumillo, "Nested median filtering for detecting T-wave offset in ECGs," *Electron. Lett.*, vol. 38, no. 14, pp. 682–683, Jul. 2002.
[18] J. P. Martínez, R. Almeida, A. P. Rocha, P. Laguna, and S. Olmos, "Stability of QT measurements in the PTB database depending on the selected lead," in *Proc. Comput. Cardiol. Conf. 2006*, vol. 33, pp. 341–344.
[19] R. Almeida, J. P. Martínez, A. P. Rocha, and P. Laguna, "QRS complex boundaries location for multilead electrocardiogram," in *Proc. Comput. Stat. 2008, Int. Assoc. Stat. Comput. Symp.*, Heidelberg, Germany: Physica-Verlag, 2008, pp. 447–454.
[20] R. Sameni, C. Jutten, and M. B. Shamsollahi, "What ICA provides for ECG processing: Application to noninvasive fetal ECG extraction," in *Proc. 2006 IEEE Int. Symp. Signal Process. Inf. Technol.*, pp. 656–661.
[21] T. He, G. Clifford, and L. Tarassenko, "Application of independent component analysis in removing artefacts from the electrocardiogram," *Neural Comput. Appl.*, vol. 15, no. 2, pp. 105–116, 2006.
[22] J. L. Willems, P. Arnaud, J. H. van Bemmel, P. J. Bourdillon, R. Degani, B. Denis, I. Graham, F. M. Harms, P. W. Macfarlane, G. Mazzocca, J. Meyer, and C. Zywietz, "Principal component analysis in ECG signal processing," *EURASIP J. Adv. Signal Process.*, vol. 2007, pp. 74580-1–74580-21, 2007.

Rute Almeida was born in Porto, Portugal, in 1979. She received mathematics applied to technology degree, in 2000, and the Ph.D. degree in applied mathematics, in 2007, both from the Faculty of Sciences, University of Porto (FCUP), Porto, Portugal.

Between March and October 2001, she was with the Autonomic Function Study Center, Hospital S. João, where she worked on methods for automatic delineation of the ECG. From October 2001 to September 2005, she was supported by an individual grant from the Foundation for Science and Technology (Portugal) and the European Social Fund. Since 2005, she has been a member of the Centro de Matemática da Universidade do Porto (CMUP), Porto. Since 2007, she has been a Researcher at the Spanish Center for Biomedical Engineering, Biomaterial and Nano-medicine Research Centro de Investigación Biomédica en Red en Bioingeniería, Biomateriales y Nanomedicina (CIBER-BBN), under protocol with the University of Zaragoza (UNIZAR), Zaragoza, Spain. She is also with the Aragón Institute for Engineering Research (I3A) at UNIZAR. Her current research interests include time-scale methods and the automatic analysis of the ECG, namely the study of ventricular repolarization.

Juan Pablo Martínez was born in Zaragoza, Spain, in 1976. He received the M.S. degree in telecommunication engineering and the Ph.D. degree in biomedical engineering from the University of Zaragoza (UZ), Zaragoza, in 1999 and 2005, respectively.

Since 2000, he has been an Assistant Professor in the Department of Electronic Engineering and Communications, UZ, where he has been an Associate Professor since 2007. He is a Researcher at the Aragón Institute for Engineering Research (I3A), and is also with the Centro de Investigación Biomédica en Red en Bioingeniería, Biomateriales y Nanomedicina (CIBER-BBN). His current research interests include the field of biomedical signal processing, including signals of cardiovascular origin.

Ana Paula Rocha (M'05) was born in Coimbra, Portugal, in 1957. She received the Appl. Math. degree and the Ph.D. degree in applied mathematics, systems theory, and signal processing from the Faculty of Sciences, University of Porto (FCUP), Porto, Portugal, in 1980 and 1993, respectively.

She is currently an Auxiliar Professor in the Department of Applied Mathematics, FCUP, where she is also a member of the Centro de Matemática da Universidade do Porto. Her current research interests include biomedical signals and system analysis (EMG, cardiovascular systems analysis, and autonomic nervous system characterization), time–frequency/time-scale signal analysis, point processes spectral analysis, data treatment, and interpretation.

Pablo Laguna (M'92–SM'06) was born in Jaca, Spain, in 1962. He received the M.S. and Ph.D. degrees in physics from the Science Faculty, University of Zaragoza, Zaragoza, Spain, in 1985 and 1990, respectively.

From 1987 to 1992, he was an Assistant Professor of automatic control in the Department of Control Engineering, Politecnic University of Catalonia (UPC), Spain, where he was also a Researcher with the Biomedical Engineering Division, Institute of Cybernetics (UPC-CSIC). From 1992 to 2005, he was an Associated Professor at the University of Zaragoza, where he is a Full Professor of signal processing and communications in the Department of Electrical Engineering, Engineering School, and also a Researcher at the Aragón Institute for Engineering Research (I3A). He is also a member of the Spanish center for Biomedical Engineering, Biomaterial and Nanomedicine Research Centro de Investigación Biomédica en Red en Bioingeniería, Biomateriales y Nanomedicina (CIBER-BBN). His current research interests include signal processing, in particular applied to biomedical applications. He is a coauthor of *Bioelectrical Signal Processing in Cardiac and Neurological Applications* (Elsevier, 2005).